We are IntechOpen, the world's leading publisher of Open Access books
Built by scientists, for scientists

6,900
Open access books available

185,000
International authors and editors

200M
Downloads

154
Countries delivered to

Our authors are among the

TOP 1%
most cited scientists

12.2%
Contributors from top 500 universities

BOOK CITATION INDEX
CLARIVATE ANALYTICS
INDEXED

WEB OF SCIENCE™

Selection of our books indexed in the Book Citation Index
in Web of Science™ Core Collection (BKCI)

Interested in publishing with us?
Contact book.department@intechopen.com

Numbers displayed above are based on latest data collected.
For more information visit www.intechopen.com

Longshore Sediment Transport Measurements on Sandy Macrotidal Beaches Compared with Sediment Transport Formulae

Adrien Cartier, Philippe Larroudé and
Arnaud Héquette

Additional information is available at the end of the chapter

1. Introduction

In a context of global climate change, local sea level rise could affect the different coastal processes as erosion, transport and deposition which are responsible in maintaining the coastline. The study of sediment transport processes is one of the key for a better understanding of the coastal evolution which is needed for effective design of coastal engineering or to protect anthropogenic activities and population from marine submersion. One of the main processes that control coastal evolution is sediment transport. A number of studies have been focused on this topic, but they were mostly restricted to micro- to mesotidal beaches [1-3] and field investigations on sandy macrotidal beaches appear to be more limited, notably because these environments are less common along the worldwide coastline [4].

Only a few studies have been conducted for quantifying sediment flux on macrotidal beaches [5, 6] where sediment transport results from the complex interactions of tidal currents with longshore currents generated by obliquely incident breaking waves, this complexity being further increased by the large variations in water level that induce significant horizontal translations of the surf zone. Although a number of studies were recently conducted on the morphodynamics of the barred macrotidal beaches of Northern France [7-12], relatively little effort has been dedicated to measuring longshore sediment transport on these beaches, even though it is largely recognized that they are affected by significant longshore transport that plays a major role in the morphodynamics of the intertidal zone [10, 13]. Apart from some attempts to make estimates of longshore sediment transport from fluorescent tracers [10, 14-16] and to infer transport directions using grain-size trend analysis techniques [17,

INTECH
open science | open minds

18] no studies were conducted up to now for trying to quantify accurately longshore sand transport on these sandy macrotidal beaches.

Very recent field experiments conducted on macrotidal beaches of Northern France showed that, at a very short time scale (minutes), cross shore sediment flux is generally higher than longshore flux, suggesting that shore-perpendicular sediment transport associated with wave oscillatory currents probably represents a major factor controlling the cross-shore migration of intertidal bars [19]. Further analysis highlighted the strong dependence of longshore sediment transport (LST) on instantaneous hydrodynamic conditions that are extremely variable from one hydrodynamic zone to the other, notably between the non-breaking zone of wave shoaling and the surf zone [20]. Although such field experiments can provide very useful results that contribute to a better understanding of beach morphodynamic and sediment transport dynamics, *in situ* experiments are hard to undertake due to a series of technical and environmental factors. During the last decades, numerical modeling of coastal sediment transport and morphodynamics has grown substantially and is now largely used by the coastal scientific community. As a first step, models have to be calibrated in order to correspond as close as possible to natural phenomenae. Thus, a major focus of nearshore research is to relate (measured and predicted) sediment transport rates to morphological change, with the aim of improving our understanding and modeling capabilities of beach morphodynamics.

This study is based on previous field investigations conducted on sandy barred macrotidal beaches of northern France by Cartier and Héquette [19-22] during which longshore sediment fluxes were estimated using streamer traps, following the method proposed by Kraus [23]. Longshore sediment transport rates were compared with several sediment transport formulae integrated in a numerical model. This numerical model is characterized by a coupling of three codes consisting in enchained Artemis for swells, Telemac2d for the currents and Sisyphe for the morphodynamic evolution [24]. The aim of this contribution is to present the results of the field measurements carried out on these multi-barred sandy beaches and to discuss the abilities of numerical models to predict longshore sediment transport on these macrotidal environments.

2. Study area

This study has been conducted on three sandy barred beaches of Northern France from November 2008 to March 2010. The first field experiment site (Zuydcoote, ZY) is located near the Belgian border, facing the North Sea; the second site (Wissant Bay, WI) is on the shore of the Dover Strait, while the third study site (Hardelot, HA) is located on the eastern English Channel coast (Figure 1).
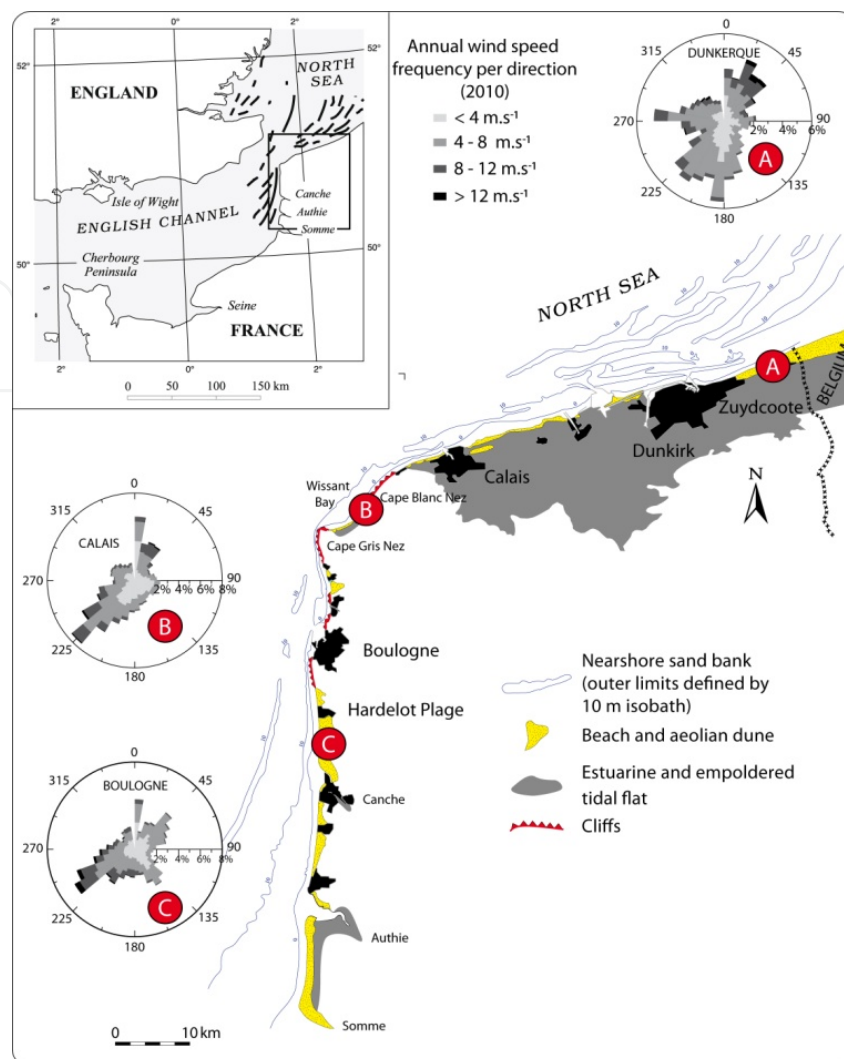
Figure 1. Location of the three study sites along the coast of Northern France: A) Zuydcoote; B) Wissant Bay; C) Hardelot Beach.

The study sites consist of 300 to 800 m wide dissipative beaches characterized by extensive intertidal bar-trough systems (Figure 2). The coasts of Northern France are exposed to relatively low-energy waves that are refracted by numerous offshore sand banks. Dominant wave directions are from southwest to west, originating from the English Channel followed by waves from the northeast to north, generated in the North Sea. Offshore modal significant wave heights are similar for all the study sites and are less than 1.5 m, but may exceed 4 m during storms [25, 26]. The presence of several sand banks on the shoreface and the inner shelf and the gentle beach slopes that characterize the coasts of Northern France are responsible for strong wave energy dissipation, resulting in modal significant wave heights lower than 0.6 m in the intertidal zone [11, 25]. Wave heights can nevertheless reach 2 m on the foreshore during extreme events [27]. During such high wave energy conditions, substantial volumes of sediment can be transported on these beaches as revealed by the formation and migration of large megaripples across the intertidal zone [10].
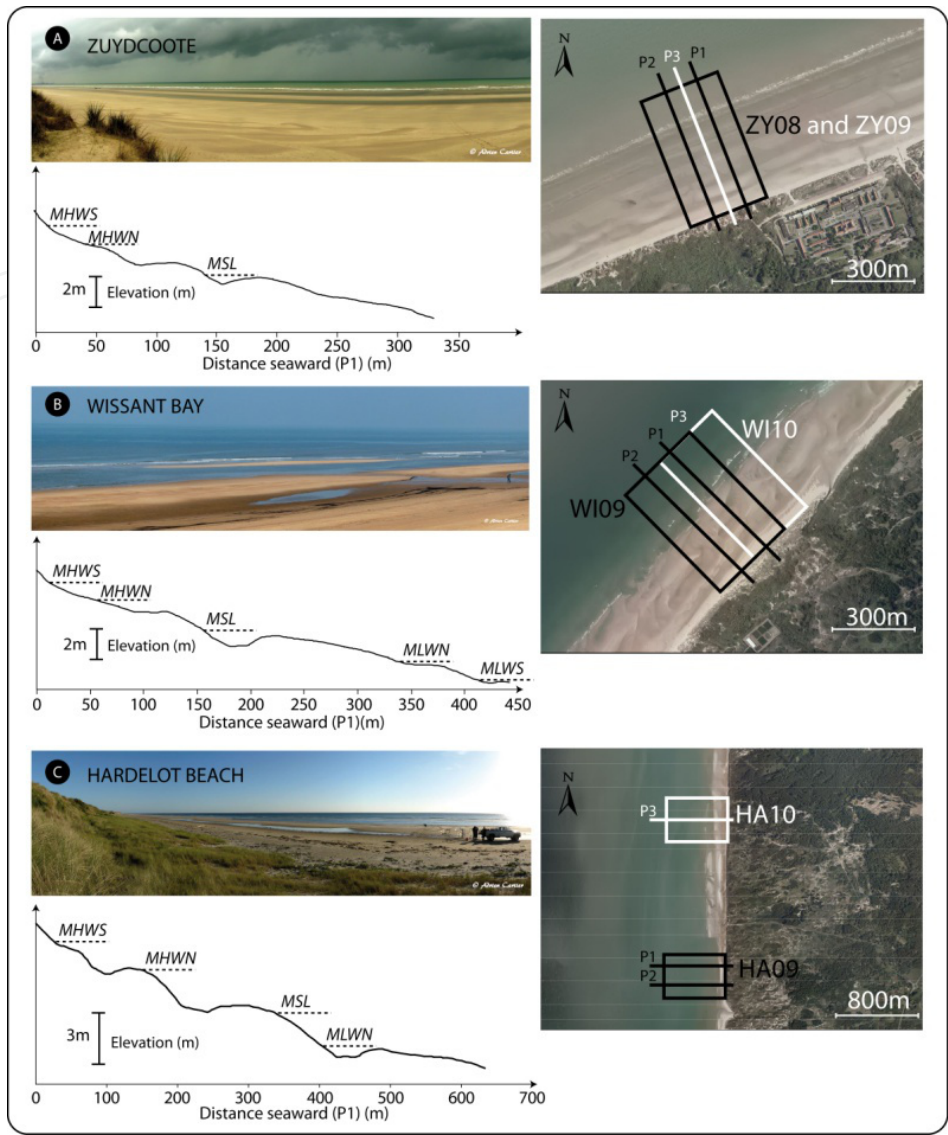
Figure 2. Shore perpendicular beach profiles, panoramic and aerial vertical photographs (©Orthophoto, 2005) of each study site (See Figure 1 for location).

The study sites are affected by semi-diurnal tides with mean spring tide ranging from about 6 m at Zuydcoote to almost 10 m at Hardelot (Figure 3). This high tidal range is responsible for relatively strong tidal currents that flow almost parallel to the shoreline in the coastal zone, at Wissant and Zuydcoote, the ebb is directed westward and the flood is flowing eastward, while at Hardelot Beach, the ebb and flood are directed southward and northward respectively. The reversing of tidal currents does not occur at high or low tide, but typically after a delay of two to three hours. Current measurements conducted in previous studies revealed that the speeds of flood currents exceed those of the ebb, resulting in a flood-dominated asymmetry responsible for a net regional sediment transport to the east-northeast [9, 28].
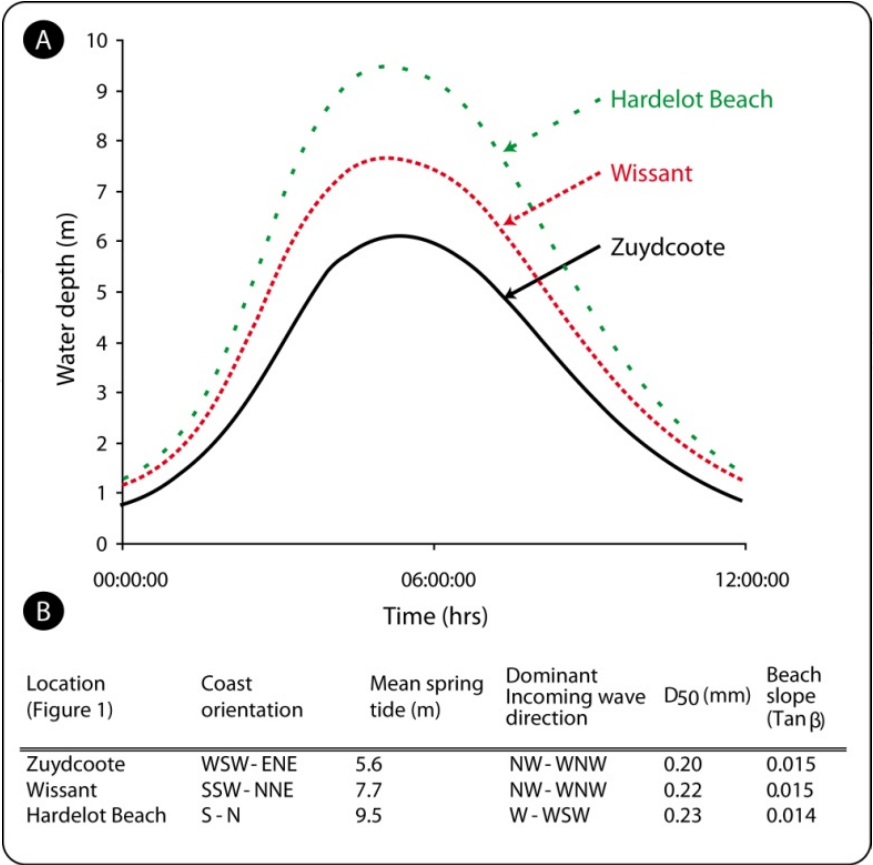
Figure 3. General characteristics of each field site. A) Water level variations for mean spring tide. B) Summary of hydrodynamic and morphodynamic characteristics at each field sites (see Figure 1 for location)

3. Field measurements

3.1. Field methodology

In order to determine the ability of numerical models to predict sediment transport and morphodynamics over sandy beds, several field measurements of sediment transport have been carried out on three different sandy macrotidal beaches. Although sediment fluxes can be estimated using acoustic or optical backscatter instruments, this study was based on direct sediment transport measurements using sediment traps rather than these techniques. Previous studies highlighted that acoustic or optical backscatter sensors can often be problematic in the coastal zone due to bubbling in the breaker and surf zones [29] and/ or to the presence of organic matter in the water column and to grain size variability [30]. Thus, streamer traps appeared to be the most adapted and the most accurate method to measure longshore sediment transport in the shoaling, breaking and surf zone on these macrotidal beaches.
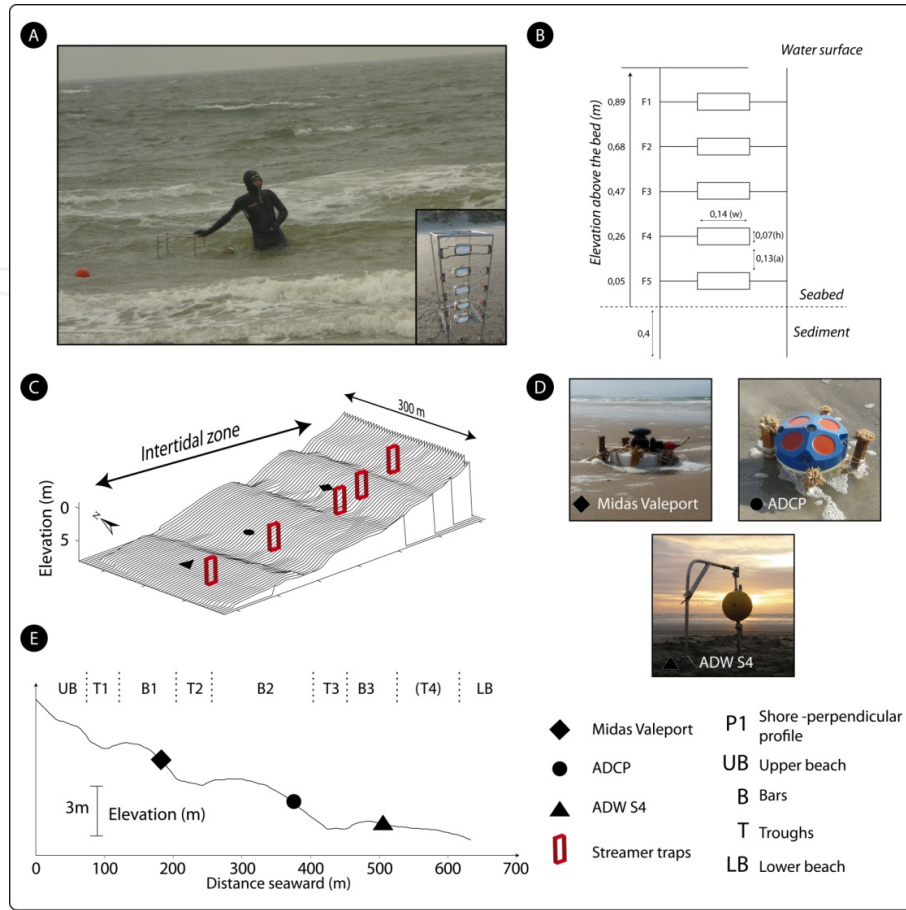
Figure 4. Field methodology. A) *In situ* measurements of longshore sediment transport during low to moderate wave energy conditions. B) Schematic representation of streamer trap used during the experiments. C) Locations of sediment trap deployment along a shore-perpendicular transect. D) Hydrographic instruments used during the field experiments. E) Shore-perpendicular profile showing the location of the hydrographic instruments. Codes refer to beach morphology where UB and LB are upper and lower beach respectively; B and T correspond to bars and troughs. Elevations are relative to the French topographic datum (IGN69).

Longshore sediment fluxes were estimated using streamer traps, following the method proposed by Kraus [23]. The sediment traps consisted of a vertical array of five individual streamer traps with 63 μm mesh size sieve cloth that collects sand-size particles at different elevations above the bed. First streamer trap (F5) is located 0.05 m above the bed and the last one (F1) is at approximately 0.90 m (Figure 4, B). Measurements of LST with the sediment traps were undertaken during 10 minutes.

Calculations of the sediment flux from sand traps were carried out according to the procedure of Rosati and Kraus [31]. The sediment flux Q(f), in kg.s^{-1}.m^{-2}, at a streamer trap (f) is equivalent to:

$$Q(f) = \frac{S(f)}{w * h * t}$$

Where S(f) is the dry weight of sediment collected in the streamer (f), h is the height of the streamer opening (0.07 m), w is the streamer width (0.14 m), and t is the sampling period (≈

10 minutes). The sediment flux between neighboring streamers QE(f) corresponds to the linear interpolation between two adjacent traps:

$$QE(f)=0,5*(F(f)+F(f+1))$$

The depth integrated flux (Q) in kg.s^{-1}.m^{-1} is:

$$Q=h*\sum_{i=1}^{N}Q(f)+\sum_{i=1}^{N}a(f)*QE(f)$$

Where h is the height of the streamer opening in meters, Q(f) is the sediment flux at a streamer f, a(f) is the distance between neighboring streamers, QE(f) is the sediment flux between neighboring streamers and N is the total number of streamers (N = 5).

Measurements of LST were carried out at several locations across the intertidal zone during rising and falling tides in order to obtain estimates of longshore sediment flux from the lower to the upper beach during flood and ebb (Figure 4, C).Although the sediment traps were usually deployed in similar water depths, ranging from 0.8 to 1.4 m, sediment transport measurements took place in various hydrodynamic zones including shoaling, breaker and surf zones, depending on wave activity during sampling. For safety reasons, sand transport measurements were conducted only under low to moderate wave energy conditions (H_s max ≈ 0.7 m).

Two field experiments were conducted on each study site: Zuydcoote in November 2008 (ZY08) and December 2009 (ZY09), Wissant in March 2009 (WI09) and March-April 2010, (WI10), and Hardelot in June 2009 (HA09) and January-February 2010 (HA10), resulting in the collection of 172 depth-integrated sediment flux measurements.

Coastal hydrodynamics were measured at different locations across the bar-trough morphology along cross shore transects using various hydrographic instrument (Figure 4, D). Waves and currents were measured using three different hydrographic instruments: an Acoustic Doppler Current Profiler (ADCP), and two electromagnetic wave and current meters (Midas Valeport©, and InterOcean ADW S4). All instruments operated during 9 minutes intervals every 15 minutes at a frequency of 2 Hz, providing almost continuous records of significant wave height (H_s), wave period and direction, longshore current velocity (V_l), and mean current velocity (V_m) and direction. Current velocity was measured at different elevations above the bed depending on each instrument. The ADW S4 and Valeport current meters recorded current velocity at 0.4 m and 0.2 m above seabed respectively, while the ADCP measured current velocity at intervals of 0.2 m through the water column from 0.4 m above the bed to the water surface. Current velocity at 0.2 m above the bed was estimated using the ADCP data by applying a logarithmic regression curve to the measured velocities obtained at different elevations in the water column.

Beach morphology plays a major role in the variation of sediment transport rates, especially on bar-trough topography [9, 10, 13, 32, 33]. Thus, during each field experiment, beach morphology was surveyed using a very high resolution Differential Global Positioning System (DGPS) with horizontal and vertical error margins of ± 2 cm and ± 4 cm respectively. A 300 m wide zone of the beach was systematically surveyed on each study site whereas the cross-shore extent of the surveyed area was variable depending on tidal range.

3.2. Sediment transport: role of the main physical forcings

3.2.1. Hydrodynamic conditions during the field experiments

The field experiments have been conducted under different conditions of wave energy and tidal range at each study site. Because sand transport measurements were restricted to moderate to low wave energy conditions, the range of wave heights recorded during sediment trapping is relatively constrained. A classification of wave energy conditions during the field experiments was adopted in which $H_s< 0,2$ m represents low wave energy conditions, $0,2 \leq H_s< 0,4$ m refers to moderate wave energy conditions and $H_s \geq 0,4$ m represents higher energetic conditions (Figure 5).
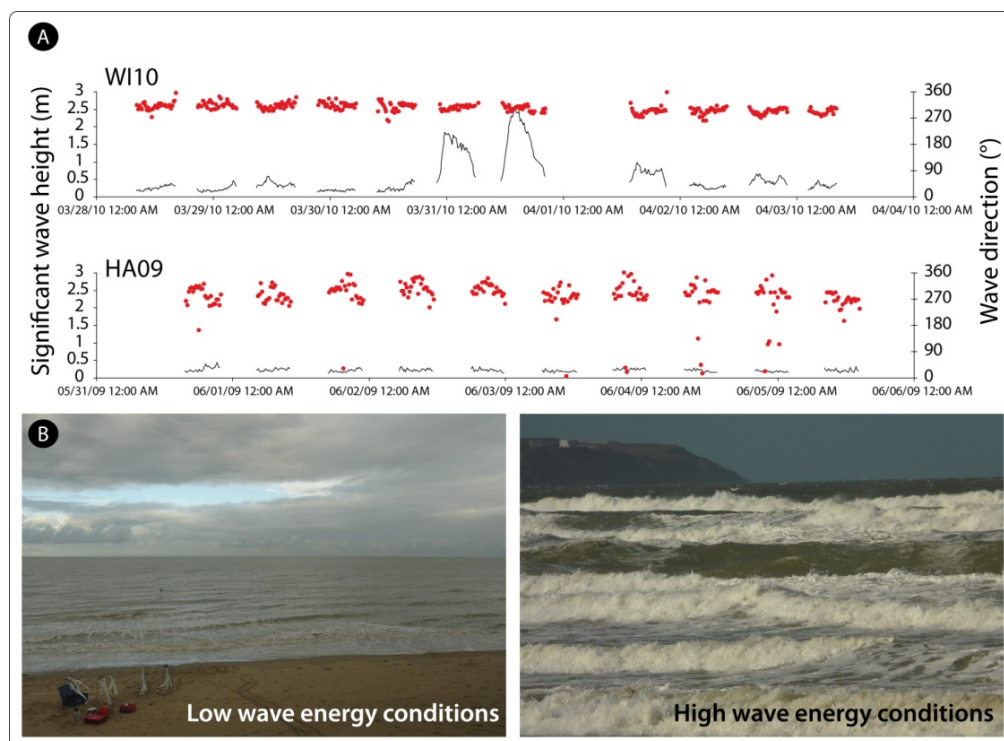

Figure 5. Examples of hydrodynamic conditions during some field experiments. A) Time series of significant wave height (m) and wave direction (°) during WI10 and HA09 experiments. B) Photographs of low and high wave energy conditions during the experiments.

The lowest wave energy conditions took place during the HA09 experiment. 99% of the significant wave heights were under 0.4 m and 46% were under 0.2 m for a mean longshore current velocity of 0.2 m.s⁻¹. High wave energy conditions occurred during several field experiments with a maximum wave height of 2.4 m reached at Wissant in 2010 (WI10) while longshore current velocity reached 2 m.s⁻¹. Such high energy conditions lasted over only two tidal cycles however during this field experiment (Figure 5). In comparison, the maximum significant wave height during the HA10 experiment was 2.1 m, but the duration of high energy conditions was considerably longer as 80% of the recorded wave heights was higher than 0.4

m for an average H_s of 0.70 m, which is remarkably high for the relatively low-energy coasts of Northern France where wave heights are generally lower in the intertidal zone [11, 13].

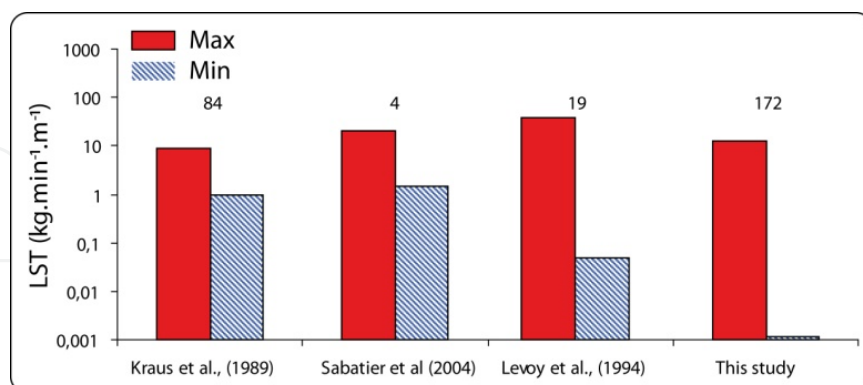### 3.2.2. Longshore sediment transport rates

During the six field experiments, more than 700 sediment samples were collected, which were used to compute 172 depth-integrated sediment fluxes. Among these, 79 depth-integrated sediment fluxes were obtained close to a hydrographic instrument, allowing a comparison between LST and hydrodynamic parameters. Throughout the 6 field experiments, most of the longshore sediment transport rates (> 50%) ranged from 1×10^{-4} kg.s^{-1}.m^{-1} to 1×10^{-3} kg.s^{-1}.m^{-1} (Figure 6A). Sediment transport rates show a high variability depending on the study site and during each field experiment due to variations in hydrodynamic conditions (Figure 6B). Longshore sediment flux reached values up to 2.1×10^{-1} kg.s^{-1}.m^{-1} during the ZY09 experiment, which was the most energetic event during which sediment sampling took place. Lower rates of sediment transport were measured in the vicinity of current meters where sediment flux nevertheless reached approximately 1.6×10^{-1} kg.s^{-1}.m^{-1} for a mean flow velocity of 0.5 m.s^{-1}. Significantly higher transport rates were observed during the most energetic conditions, however, notably during the HA10, ZY09 and WI09 field experiments (Figure 6B).
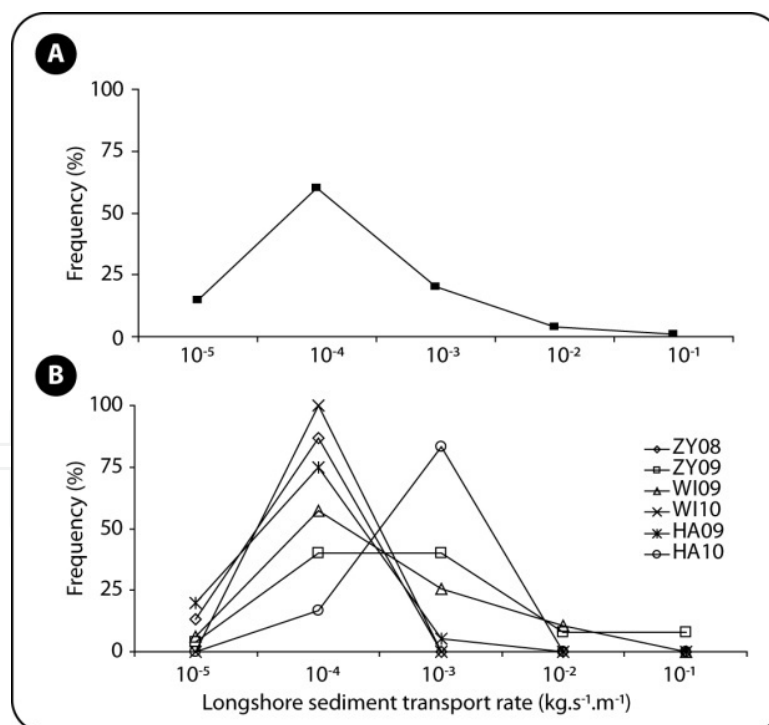
Figure 6. Range of LST for (A) all field experiments and (B) each field experiment.

Longshore sediment transport rates measured during this study are in the same order of magnitude as other studies conducted on microtidal beaches [23, 31, 34-37] as well as on macrotidal beaches [5] (Figure 7). The fact that ranges of values are similar whatever the ti-

dal conditions are, suggests that tidally-induced currents are not the main forcing and do not act significantly on longshore sediment transport magnitude.

Figure 7. Maximum and minimum values of LST measured using streamer traps on microtidal beaches[35, 38] and macrotidal beaches [5]. Numbers of samples are located just above the bar charts.
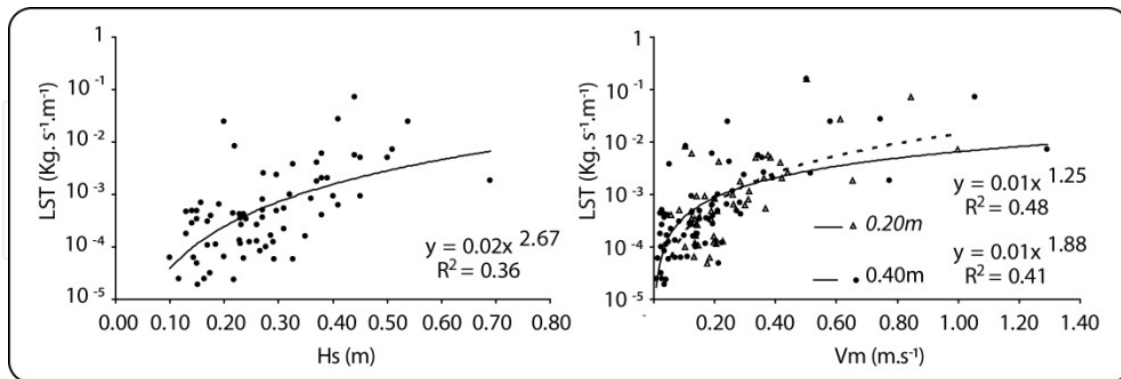
3.2.3. Relationship between longshore sediment transport and hydrodynamics

Comparisons of transport rates with hydrodynamic data showed that longshore sediment transport increases with both significant wave height and mean current velocity (Figure 8). Low sediment transport ($< 1.0 \times 10^{-4}$ kg.s^{-1}.m^{-1}) is mainly associated with small wave heights (< 0.3 m), but only a small increase in wave height appears to induce significantly larger sediment transport. However, high sediment transport values can also be associated with low wave conditions, such as during the WI09 experiment when a sediment transport rate of 2.4×10^{-2} kg.s^{-1}.m^{-1} was measured with a significant wave height of about 0.2 m for example. The variability in sediment flux values obtained during conditions of equivalent wave heights, and the fact that similar transport rates may be associated with different wave heights, even on the same beach and during the same field experiment (e.g., WI09), suggest that waves do not represent the only factor controlling sediment transport.

Least-square regression analyses show that longshore sediment flux is better correlated with current velocity than with wave height as revealed by higher determination coefficients (Figure 8). Similarly to what was observed with significant wave heights, high sediment transport rates can also be observed with lower current velocities. Further analysis detailed in Cartier and Héquette [20] highlighted that variations in LST are better explained by these two forcing parameters in the surf zone, where currents generated by obliquely incident breaking waves are acting, than in the shoaling zone.

Longshore sediment transport in the nearshore zone is commonly related to the longshore wave energy flux (P_l) evaluated at the breaker zone, sand transport being expressed as an immersed-weight transport rate (I_l) and related to P_l [39]. Conversely to what was observed in other studies [40], however, previous analyses of our data showed no relationship between LST and wave breaking angle, which is directly involved in the computation of P_l [19,

20, 22]. These results may be explained by the influence of tidal currents that interact with wave-induced longshore currents on these macrotidal beaches

Figure 8. Relationship between LST and significant wave height (H_s), and with mean current velocity (V_m) at 0.2 m (triangle) and 0.4 m (circles) above the bed using all the samples collected near a current meter during all field experiments.

4. Sediment transport modelling

4.1. Methodology

The methodology used during field experiments did not allow us to compare sand transport rates with well known formulae such as the CERC formula [41] or the Kamphuis's formula [42] for example. These formulations, which are essentially based on a wave energy flux approach, provide estimates of total sediment transport rates across the entire surf zone. A large amount of studies have compared that kind of numerical model with in situ measurements [29, 43-47], or with laboratory measurements [48-50], and even between several numerical models in order to understand their behaviour with virtual data [51-53]. However, our measurements can not be compared with these numerical models because sand trapping took place at only one location in the surf or shoaling zone while these formulae estimate the total longshore sediment transport across the surf zone.

There is, nevertheless, a number of sediment transport formulae that can be compared with localized measurements of sand flux. In the present study, calculations of sediment transport rates have been realized using a coupling of three codes [54]. The sedimentary evolution is modeled under the action of the oblique incident waves and is coupled with different numerical tools dedicated to the other process involved in the nearshore zone. We can mention the following modules:

The wave module takes into account the surge energy dissipation (hyperbolic equation of extended Berkhoff). The Artemis code (Agitation and Refraction with Telemac2d on a Mild Slope) solves the Berkhoff equation taken from Navier-Stokes equations with some other hypotheses (small wave steepness of the surface wave, small slope...). The main results are, for

every node of the mesh, the height, the phase and the incidence of the waves. Artemis can take into account the reflection and the refraction of waves on an obstacle, the bottom friction and the breakers. One of the difficulties with Artemis is that a fine mesh must be used to have good results whereas Telemac2d does not need such a fine mesh.

The hydrodynamic module calculates currents induced by means of the surge of the waves, from the concept of radiation constraints obtained according to the module of waves. Telemac2d is designed to simulate the free surface flow of water in coastal areas or in rivers. This code solves Barré Saint-Venant equations taken from Navier-Stokes equations vertically averaged. Then, the main results are, for every node of the mesh, the water depth and the velocity averaged over the water column. Telemac2d is able to represent the following physical phenomena: propagation of long periodic waves, including non-linear effects, wetting and drying of intertidal zone, bed friction, turbulence…

The sedimentary module integrates the combined actions of the waves and the wave currents (2D or 3D) on the transport of sediment [24].

The Sisyphe code solves the bottom evolution equation which expresses the mass conservation by directly using a current field result file given by Telemac2d (Figure 9). Several of the most currently used empirical or semi-empirical formulas are already integrated in Sisyphe.
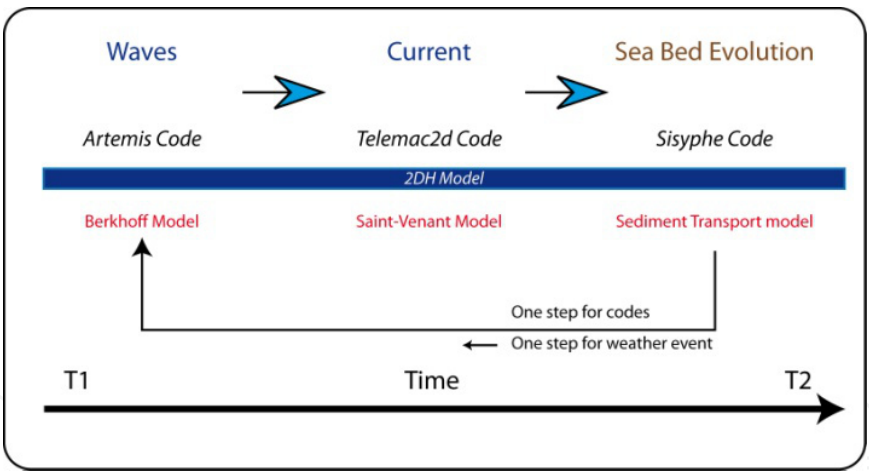
Figure 9. Diagram of the model ATS (Artemis-Telemac-Sisyphe) used in our simulations, showing the principle of external coupling to make a loop over one hydro-meteorological event time step (between t1 and t2).

A hydrodynamic simplified model (called Multi1DH) uses the following assumptions: a random wave approach and a 1DH (cross-shore) direction. An offshore wave model (shoaling + bottom friction + wave asymmetry) is used with the break point estimation. The waves in the surf zone are modeled with the classic model of Svendsen (1984) with an undertow model (roller effect) [55, 56]. The longshore current model is the Longuet-Higgins's model [57]. The model is included in the Sisyphe code to calculate the sea bed evolution with several sediment transport formulas.

It is generally accepted that the estimate is acceptable when the flux is between 0.5 and 2 times the in situ measurement [58]. Thus, in the following figures, three lines symbolize the extent of data that are significant at $0.5\ Q_{sm} < Q_{sc} < 2\ Q_{sm}$. The standard error ($S_{rms}$) was also calculated using the following equation to characterize the dispersion of data, where the higher the values, the higher the data are scattered.

$$S_{rms} = \sqrt{\frac{\sum_{i=1}^{N} \left[Log(Q_{Sc}) - Log(Q_{Sm}) \right]^2}{N-2}}$$

where Q_{sc} is the flux calculated, Q_{sm} the measured flux and N the number value.

4.2. Results

4.2.1. Potential effects of water depth

Sediment flux measurements were performed in a water depth between approximately 1 m and 1.5 m, but because of the excursion of the tide, these measurements were made at several locations on the foreshore (Figure 4). Calculation of sediment load at the same location on the field requires a lot of computer manipulations. So initially, the sediment loads are modelled in the middle of the digital domain. The water level in the middle of the simulated field rarely matches the exact water level measured during sampling. A test was therefore carried out to assess the potential effects of water depth on computed sediment flux using the data measured during the two field experiments at Hardelot beach (2009 and 2010). For the numerical simulations, bathymetry has been considered as stable during and between the two field campaigns.

The following graphs show the control of the water level on the accuracy of modeled flux (Figure 10). The example shows calculations based on the expression of Bijker [59], similar observations having been observed for the other formulations.

The results show that sediment fluxes tend to be better estimated with decreasing water depth, which is consistent with the depths at which measurements were made. The correlations are even better for water depths just below the water level of the in situ measurement (<1 m). In a water depth between 2.70 m and 1.74 m, the computed values seem to line up around $1 \times 10^{-3} kg.s^{-1}.m^{-1}$. There is very little change in calculated flux in comparison with those measured in situ. As soon as the water level is similar to that of measurement at the time of trapping (1.51 m), the distribution of points tends to align the right $Q_{sc} = Q_{sm}$. However, when the water column is much lower than reality, many errors appear in the calculation and the estimation of sediment flux becomes completely erroneous. In fact, the RMS errors are quite high when the water level is far from the actual water depth (Figure 10). It should be emphasized, however with all the initial approximations, the mere fact of positioning the water level at the same level as during the sampling resulted in relatively better results. In particular, when h = 0.91 m, which resulted in a percentage of acceptable values of 32%. Overall calculated sediment fluxes are nevertheless generally overestimated.
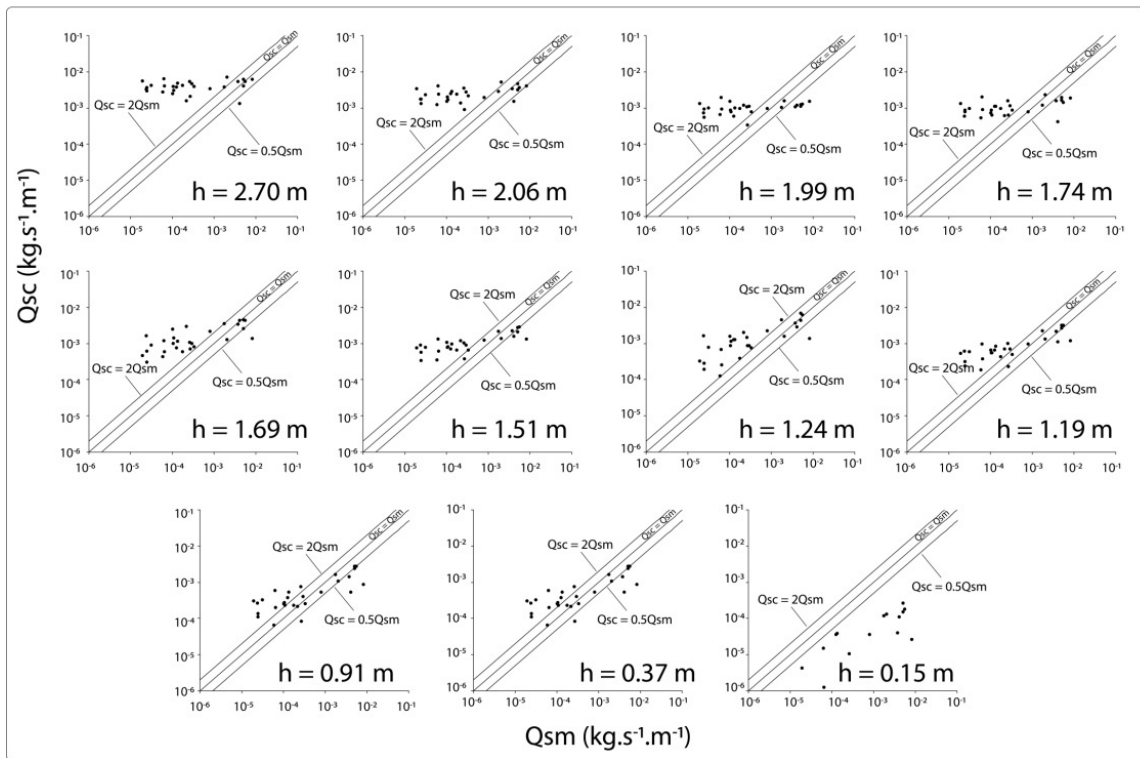
Figure 10. Comparison between measured (Q_{sm}) and computed (Q_{sc}) transport rates using Bijker's formula [59] for different water depths (h).

The water level acts directly on the current profile and associated sediment transport mechanisms. Thus, when the water column is higher than that at the time of measurement, the transport in suspension is favoured in the modelling, leading to an overestimation of the integrated flux in the water column. In contrast, a shallower water column could lead to higher sediment fluxes due to increased bed shear. However, it appears that the formulas are struggling to express sediment transport in very shallow water. Despite very simplified initial conditions, the results obtained in this study show that the coupling of these three codes is not so far from reality when we take into account the water level measured in situ. More precise calibrations will likely improve the accuracy of the results in the future.

4.2.2. Calculated sediment flux against in situ data

Using the water levels measured during the field experiments, the calculations of sediment transport were calibrated for each case to be as close as possible to the in situ measurement. Sediment transport modeling was carried out on the beaches of Wissant and Hardelot, and sediment loads calculated by several formulas have been extracted and compared to field data. The calculations concerning the Zuydcoote field site are not presented because of problems related to the computational domain. Because the bathymetry input was not broad enough, the waves spread by the code Artemis underwent many artifacts and measurement errors that did not allow reliable sediment transport calculations.

Sediment fluxes were compared with the expressions of Bijker [59], noted BI68, and a coupling of Van Rijn formula [60] with an expression modelling the transport in suspension [61], this coupling being called the Soulsby-Van Rijn formula noted SVR97 (Figure 11). The reader is referred to [58, 62]for details on the different formulae.
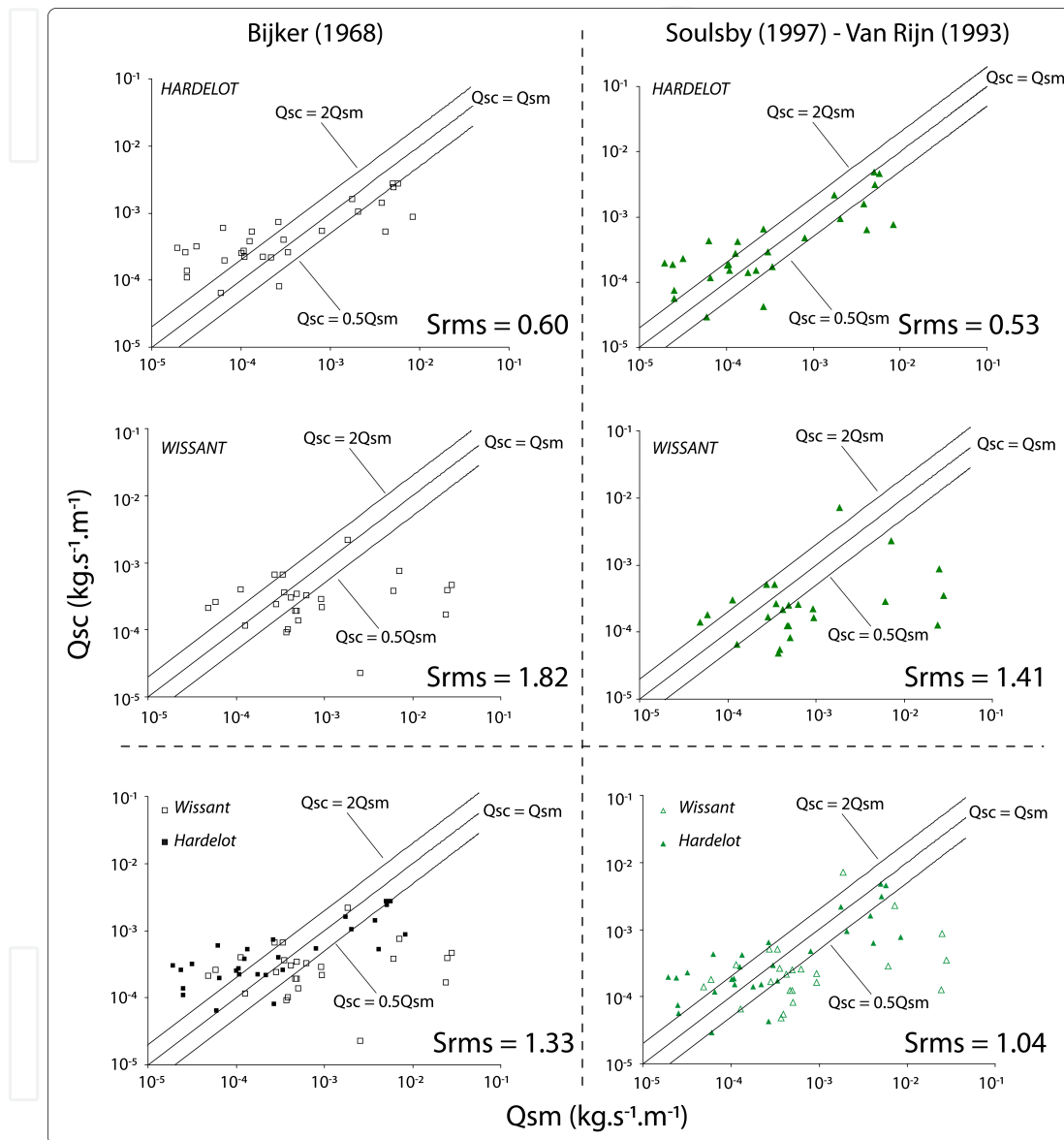
Figure 11. Comparisons between in situ (Q_{sm}) sand transport rates measured during HA09, HA10, WI09 and WI10, with calculated sediment fluxes (Q_{sc}) following Bijker and Soulsby – Van Rijn formulae.

The results were analyzed according to the study site and the mathematical expression used. The results are better on the site of Hardelot for both formulas, the error S_{rms} being less than 1.0 with a minimum of 0.53 with SVR97. Moreover, the percentage of significant values reaches 32% and 46% for SVR97 and BI68, respectively. On the site of Wissant, it does not exceed 30% whatever the formula. RMS errors are associated with a greater dispersion of

data readily observable in the graphs (Figure 11). When considering all the data, the formula for SVR97 is the expression that is most satisfactory with a S_{rms} of only 1.04 and 36% of acceptable values. The proportion of sediment flux of low intensities ($<1 \times 10^{-3}$ $kg.s^{-1}.m^{-1}$) is higher during the campaigns carried out in Hardelot than those held in Wissant. Conversely, the flux measurements acquired during the field investigations in the Bay of Wissant proved to be higher. Morphological changes were also more significant in Wissant than during the campaigns conducted in Hardelot.

5. Discussion

In the present study, measurements of sediment flux were carried out at successive positions between the lower and the upper beach during rising or falling tide in order to measure sediment transport in comparable water depths. Our results showed that sand transport was mainly dependent on the mean flow, especially above a velocity threshold of approximately 0.4 $m.s^{-1}$ (Figure 8). Further results have shown that sediment transport was also controlled by wave action, but correlation analyses between LST and significant wave height showed a better relationship in the surf zone than in the non-breaking zone [20]. These observations highlight the mere fact that sediment transport processes are strongly different from a hydrodynamic zone to another and it underlines the need to use appropriate formulae in order to model sediment transport properly. Although a large amount of studies compared sediment transport calculation against in situ data, few of them have been undertaken using sediment transport measurements from macrotidal beaches.

Results obtained in a previous study by Camenen and Larroudé [62] showed that the Bijker formula generally tends to underestimate the sediment transport when there is interaction of waves and current, which is generally the case in the coastal zone. In this formula, the swell is considered to be the only mechanism responsible for suspending sediment. Therefore, when wave height is low, the simulated sediment transport remains insignificant even if the average current velocity is high. Although the strength of currents in the intertidal zone is usually related to the conditions of agitation, it may sometimes be forced by wind or induced by the combination of tidal currents and those generated by the incident swell [10]. The suspended particles are then provided by currents and waves. Our results show, however, that the higher sediment fluxes ($> 1 \times 10^{-3}$ $kg.s^{-1}.m^{-1}$) are underestimated, which may be due to low wave height and mean current that are powerful enough to induce substantial sediment transport, which cannot be modeled by this expression. Conversely, the lowest sediment transport rates occur when the swell and the mean current are of low intensity. The direction of tidal currents is also directly involved in the magnitude of the sediment flux since it can easily reduce or conversely increase wave-induced currents, depending on the phase of the tidal cycle and the direction of the longshore current. Such types of case are not considered in the model, however, which may explain a part of the variability observed between measured and computed sediment fluxes.

The formula of Soulsby-Van Rijn comes from the coupling of the Van Rijn formula [60] with an expression modeling the transport in suspension. It takes into account many physical parameters for estimating the bed load and suspended load. Even though the calculations are more complicated and time consuming, the estimate is generally better, but significant errors may occur when the wave direction is opposite to that of the current [62].

In this study, the results are particularly satisfactory for the data obtained during the field experiments at Hardelot (Figure 11) where beach morphology changes were more limited than at Wissant. When taking into account all values, it clearly appears that the most significant fluxes can nevertheless be largely underestimated since some values may be up to four times lower than the measured transport rates. During high wave energy conditions, beach morphology and bed roughness change rapidly due to an increase in bed load sediment transport. The impact of these bottom changes on the distribution of sediment in the water column is crucial and plays an important role in the mechanisms of suspended sediment transport. Because bed roughness is variable, largely depending on the local morphology of the beach, it is necessary to incorporate changes in beach morphology in the process of calculation which has not been done yet in this first attempt to model longshore transport on macrotidal beaches.

6. Conclusion

Despite several simplifications in the modeling procedure, comparisons of longshore sediment transport fluxes measured on sandy macrotidal beaches with computed sand fluxes gave encouraging results. It was shown that water depth is one of the major parameter affecting modeled sediment transport rates, as calculated sand fluxes were more comparable with in situ measurements when simulated water depth was similar to the actual water depth measured in the field. The height of the water column therefore represents a key term to consider in modeling sediment transport on these beaches. The best modeling results were obtained with the data collected during low energy conditions at Hardelot beach where the beach morphology was the most stable. A limitation of the modeling approach used in this study is related to the fact that beach morphology changes are not taken into account in the calculations, which should be considered in future modeling studies. Because sediment traps mainly collect sediments transported in suspension, future investigations using this data set will be aimed at de-coupling suspended and bed load transport calculation in the different sediment transport formulae in order to evaluate only the suspended sediment flux, which should result in more accurate comparisons between modeled and measured sediment transport rates.

Acknowledgements

Author details

Adrien Cartier[1*], Philippe Larroudé[2] and Arnaud Héquette[3]

*Address all correspondence to: adrien.cartier@univ-littoral.fr

1 LOG - UMR CNRS 8187, University of Littoral Côte d'Opale,, France

2 LEGI-UMR 5519 UJF, University of Grenoble,, France

3 LOG - UMR CNRS 8187, University of Littoral Côte d'Opale,, France

References

[1] Wang, P., Kraus, N. C., & Davis, R. A. (1998). Total longshore sediment transport rate in the surf zone-field measurement and empirical predictions. *J Coast. Res.*, 14, 269-282.

[2] Bayram, A., Larson, M., Miller, H. C., & Kraus, N. C. (2001). Cross-shore distribution of longshore sediment transport: comparison between predictive formulas and field measurements. *Coast. Eng.*, 44(2), 79-99.

[3] Kumar, V. S., Anand, N. M., Chandramohan, P., & Naik, G. N. (2003). Longshore sediment transport rate-measurement and estimation, central west coast of India. *Coast. Eng.*, 48, 95-109.

[4] Davies, A. G. (1980). Geographical variations in coastal development. London, Long-man, 212.

[5] Levoy, F., Montfort, O., & Rousset, H. (1994). Quantification of longshore transport in the surf zone on macrotidal beaches. Fields experiments along the western coast of Cotentin (Normandy, France). Paper presented at 24 th International Conference on Coastal Engineering., Kobé, Japon. 2282-2296.

[6] Corbau, C., Ciavola, P., Gonzalez, R., & Ferreira, O. (2002). Measurements of Cross-Shore Sand fluxes on a Macrotidal Pocket Beach (Saint-Georges Beach, Atlantic Coast, SW France). *J. Coast. Res.* [36].

[7] Reichmüth, B., & Anthony, E. J. (2008). Dynamics of intertidal drainage channels on a multi barred macrotidal beach. *Earth Surf. Process. Landf.*, 33(1), 142 -151 .

[8] Reichmüth, B., & Anthony, E. J. (2002). The variability of ridge and runnel beach morphology: examples from Northern France. *J. Coast. Res.* [36].

[9] Anthony, E. J., Levoy, F., & Montfort, O. (2004). Morphodynamics of intertidal bars on a megatidal beach, Merlimont, Northern France. *Mar. Geol.*, 208, 73-100.

[10] Sedrati, M., & Anthony, E. J. (2007). Storm-generated morphological change and longshore sand transport in the intertidal zone of a multi-barred macrotidal beach. *Mar. Geol.*, 244, 209-229.

[11] Héquette, A., Ruz, M. H., Maspataud, A., & Sipka, V. (2009). Effects of nearshore sand bank and associated channel on beach hydrodynamics: implications for beach and shoreline evolution. *J. Coast. Res.* [56].

[12] Maspataud, A., Ruz, M. H., & Héquette, A. (2009). Spatial variability in post-storm beach recovery along a macrotidal barred beach, southern North Sea. *J. Coast. Res.* [56].

[13] Reichmüt, B., & Anthony, E. J. (2007). Tidal influence on the intertidal bar morphology of two contrasting macrotidal beaches. *Geomorphology*, 90(1- 2), 101-114.

[14] Levoy, F., Montfort, O., & Larsonneur, C. (1997). Quantification des débits solides sur les plages macrotidales à l'aide de traceurs fluorescents, application à la côte ouest du Cotentin. *Oceanol. Acta*, 20(6), 811-822.

[15] Voulgaris, G., Simmonds, D., Michel, D., Howa, H., Collins, M. B., & Huntley, D. (1998). Measuring and modelling sediment transport on a macrotidal ridge and runnel beach: an intercomparison. *J. Coast. Res.*, 14(1), 315 .

[16] Stépanian, A., Vlaswinkel, B., Levoy, F., & Larsonneur, C. (2001). Fluorescent tracer experiment on a macrotidal ridge and runnel beach : a case study at Omaha beach, North France. *Coastal dynamics'01 Lund, Suède*, 1017-1027.

[17] Reichmüth, B. (2003). Contribution à la connaissance de la morphodynamique des plages à barres intertidales: Approche expérimentale, Côte d'Opale, Nord de la France. *Thèse de doctorat Université du Littoral Côte d'Opale*, 247.

[18] Héquette, A., Hemdane, Y., & Anthony, E. J. (2008). Determination of sediment transport paths in macrotidal shoreface environments: a comparison of grain-size trend analysis with near-bed current measurements. *J. Coast. Res.*, 24, 695-707.

[19] Cartier, A., & Héquette, A. (2011). Estimation of longshore and cross shore sediment transport on sandy macrotidal beaches of Northern France. Paper presented at Proceedings Coastal sediments'11, Miami, Florida, USA. 2130-2143.

[20] Cartier, A., & Héquette, A. (2011). *Longshore and cross shore variation in sediment transport on barred macrotidal beaches, Northern France.*

[21] Cartier, A. (2011). Evaluation des flux sédimentaires sur le littoral du Nord Pas-de-Calais: Vers une meilleure compréhension de la morphodynamique des plages macrotidales. *Thèse de Doctorat, Université du Littoral Côte d'Opale*.

[22] Cartier, A., & Héquette, A. (2011). Variation in longshore sediment transport under low to moderate conditions on barred macrotidal beaches. *J. Coast. Res.* [64], 45 -49 .

[23]   Kraus, N. C. (1987). Application of portable traps for obtaining point measurements of sediment transport rates in the surf zone. *J. Coast. Res.*, 3, 139-152.

[24]   Hervouet, J. M. (2007). Hydrodynamics of Free Surface Flows: Modelling With the Finite Element Method. John Wiley & Sons, 360, 10.1002/9780470319628.

[25]   Clique, P. M., & Lepetit, J. P. (1986). Catalogue sédimentologique des côtes françaises, côtes de la Mer du Nord et de la Manche. 133.

[26]   Ruz, M. H., Héquette, A., & Maspataud, A. (2009). Identifying forcing conditions responsible for foredune erosion on the northern coast of France. *J. Coast. Res.* [56].

[27]   Maspataud, A., Idier, D., Larroudé, Ph., Sabatier, F., Ruz, M. H., Charles, E., Lecacheux, S., & Héquette, A. (2010). L'apport de modèles numériques pour l'étude morphodynamique d'un système dune-plage macrotidal sous l'effet des tempêtes : plage de la dune Dewulf, Est de Dunkerque, France. XIèmes. *Journées Nationales Génie Civil-Génie Côtier Les Sables d'Olonne*, 353-360.

[28]   Héquette, A., Hemdane, Y., & Anthony, E. J. (2008). Sediment transport under wave and current combined flows on a tide-dominated shoreface, northern coast of France. *Mar. Geol*, 249, 226-242.

[29]   Esteves, L. S., Lisniowski, M. A., & Wiliams, J. J. (2009). Measuring and modelling longshore sediment transport. *Est. Coast. Shelf Sci.*, 83, 47-59.

[30]   Battisto, G. M., Friedrichs, C. T., Miller, H. C., & Resio, D. T. (1999). Response of OBS to mixed grain-size suspensions during Sandyduck'97. *Coastal sediment 99 Long Island, New York*, 1, 297-312.

[31]   Rosati, J. D., & Kraus, N. C. (1989). Development of a portable sand trap for use in the nearshore Department of the army, U.S. Corps of Engineers. *Technical report CERC* [89-91], 181.

[32]   Sipka, V., & Anthony, E. J. (1999). Morphology and Hydrodynamics of a macrotidal ridge and runnel beach under modal low conditions. *J. Res. Oceanogr.*, 24, 25-31.

[33]   Cartier, A., Larroudé, Ph, & Héquette, A. (2012). Comparison of sediment transport models with in-situ sand flux measurements and beach morphodynamic evolution. ICCE, Santander 2012. Submitted

[34]   Kraus, N. C., & Dean, J. L. (1987). Longshore sediment transport rate distributions measured by trap. *Coastal sediment'87 ACE*, 881-898.

[35]   Kraus, N. C., Gingerish, K. J., & Rosati, J. D. (1989). Duck 85 surf zone sand transport experiment. *US Army Corps of Engineers, Waterways Experiment Station, Coastal Engineering Research Center, Vicksburg, Mississippi.*, 48.

[36]   Sabatier, F. (2001). Fonctionnement et dynamiques morpho-sédimentaires du littoral du delta du Rhone. *Thèse de Doctorat Université Aix-Marseille III*.

[37]   Sabatier, F., Stive, M. J. F., & Pons, F. (2004). Longshore variation of depth of closure on a micro-tidal wave-dominated coast. Paper presented at International Conference of Coastal Engineering American Society of Civil Engineering, Lisboa. 2329-2339.

[38]   Sabatier, F., Samat, O., Chaibi, M., Lambert, A., & Pons, F. (2004, 7-9 septembre 2004). Transport sédimentaire de la dune à la zone du déferlement sur une plage sableuse

soumise à des vents de terre. Paper presented at VIIIèmes Journées Nationales Génie Civil- Génie Côtier Compiègne,. 223-229.

[39] Komar, P. D. (1998). Beach processes and sedimentation. *Pearson Education*, 544.

[40] Komar, P. D., & Inman, D. L. (1970). Longshore sand transport on beaches. *Journal of Geophysical Research*, 75(30), 5514-5527.

[41] Manual, S. P. (1984). Coastal engineering Research Center, in: U.S Army Corps of Engineers, t.E.W., DC 20314 (Ed.).

[42] Kamphuis, J. W., Davies, M. H., Nairn, R. B., & Sayao, O. J. (1986). Calculation of littoral sand transport rate. *Coast. Eng.*, 10, 1-21.

[43] Davies, A. G., Ribberink, J., Temperville, A., & Zyserma, J. A. (1997). Comparisons between sediment transport models and observations made in wave and current flows above plane beds. *Coast. Eng.*, 31, 163-198.

[44] Miller, H. C. (1999). Field measurements of longshore sediment transport during storms. *Coast. Eng.*, 36, 310-321.

[45] Eversole, D., & Fletcher, C. H. (2002). Longshore sediment transport rates on a reef-fronted beach: field data and empirical models Kaanapali Beach, Hawaii. J. Coast. Res. In press, 19.

[46] Zengh, J., & Hu, J. (2003, November 9-11). Calculation of longshore sediment transport in Shijiu Bay. Paper presented at International Conference on Estuaries and Coasts,, Hangzhou, China.

[47] Rogers, A. L., & Ravens, T. M. (2008). Measurement of Longshore Sediment Transport Rates in the Surf Zone on Galveston Island, Texas. *J. Coast. Res.* [2], 62-73.

[48] Smith, E. R., & Wang, P. (2001). Longshore sediment transport as a function of energy dissipation. Paper presented at ASCE Conf. Proc. Ocean Wave Measurement and Analysis.

[49] Wang, P., Ebersole, B. A., Smith, E. R., & Johnson, B. D. (2002). Temporal and spatial variations of surf-zone currents and suspended sediment concentration. *Coast. Eng.*, 46, 175-211.

[50] Singh, A. K., Deo, M. C., & Kumar, V. S. (2007). Prediction of littoral drift with artificial neural networks. *Hydro. Earth Syst. Sciences Disc.*, 4, 2497-2519.

[51] Schoonees, J. S., & Theron, A. K. (1995). Evaluation of10 cross-shore sediment transport morphological models. *Coast. Eng.*, 25, 1-41.

[52] Davies, A. G., van Rijn, L. C., Damgaard, J. S., van de Graaff, J., & Ribberink, J. S. (2002). Intercomparison of research and practical sand transport models. *Coast. Eng*, 46(1), 1-23.

[53] Van Maanen, B., Ruiter, d. P. J., & Ruessink, B. G. (2009). An evaluation of two alongshore transport equations with field measurements. *Coast. Eng.*, 56, 313-319.

[54] Larroudé, Ph. (2008). Methodology of seasonal morphological modelisation for nourishment strategies on a Mediterranean beach. *Mar. Pollut. Bull.*, 67, 45-52.

[55] Dally, W. R., Dean, J. L., & Dalrymple, R. A. (1984). A model for breaker decay on beaches. Paper presented at In 19th Coastal Engineering Conference Proceedings. 82-88.

[56] Svendsen, I. A. (1984). Mass flux and undertow in the surf zone. *Coast. Eng.*, 8, 347-365.

[57] Longuet-Higgins, M. S. (1970). Longshore currents generated by obliquely Incident waves 1. *Journal of Geophysical Research*, 75, 6778-6789.

[58] Camenen, B. (2003). Comparison of sediment transport formulae for the coastal environment. *Coast. Eng.*, 48, 111-132.

[59] Bijker, E. (1968). Littoral drift as function of waves and current. Paper presented at Coastal Engineering Conference Proceedings, London, UK. 415-435.

[60] Van Rijn, L. C. (1993). *Principles of sediment transport in rivers, estuaries and coastal seas.*, Publ. Aqua Publications, Zwolle, the Netherlands.

[61] Soulsby, R. (1997). *Dynamics of marine sands, a manual for practical applications.*, Thomas Telford,, Wallingford, England.

[62] Camenen, B. (2000). Numerical comparison of sediment transport formulae. Sand-wave Dynamics Workshop Lille, France. , 37-42.